water

MDPI

Article

Experimental Investigation on Bragg Resonant Reflection of Waves by Porous Submerged Breakwaters on a Horizontal Seabed

Wei Xu [1,2], Chun Chen [3,4,5,*], Min Han Htet [6], Mohammad Saydul Islam Sarkar [7], Aifeng Tao [1,2,*], Zhen Wang [1,2], Jun Fan [1,2] and Degang Jiang [3,4,5]

1 Key Laboratory of Ministry of Education for Coastal Disaster and Protection, Hohai University, Nanjing 210098, China
2 College of Harbour, Coastal and Offshore Engineering, Hohai University, Nanjing 210098, China
3 Island Research Center, Ministry of Natural Resources, Pingtan 350400, China
4 Fujian Provincial Key Laboratory of Island Conservation and Development, Island Research Center, Ministry of Natural Resources, Pingtan 350400, China
5 Observation and Research Station of Island and Coastal Ecosystem in the Western Taiwan Strait, Ministry of Natural Resources, Xiamen 361005, China
6 Department of Marine Engineering, Myanmar Maritime University, Thilawa 11293, Myanmar
7 Department of Oceanography, University of Chittagong, Chittagong 4331, Bangladesh
* Correspondence: chenchun002@163.com (C.C.); aftao@hhu.edu.cn (A.T.)

Abstract: Submerged breakwaters based on Bragg resonance could be one of the measures used for mitigating marine disasters and coastal erosion in nearshore areas. Here, flume experiments were conducted to investigate the Bragg resonant reflection of waves propagating over porous submerged breakwaters. Furthermore, the influence of permeability, relative width, relative height, and section shapes of submerged breakwaters on Bragg resonant reflection were considered. This revealed that the Bragg resonant reflection coefficient increased with the decrease in permeability and increase in the relative height of submerged breakwaters. However, a slowing trend occurred when the Bragg resonant reflection coefficient peak decreased with the increase in permeability and increased with the increase in relative height. Moreover, the primary peak Bragg resonance increased with the increase in the relative width of submerged breakwaters in the range of 0.1–0.3. This was consistent with the numerical results of Ni and Teng (2021), to a certain extent, as the reflection coefficient first increased and then decreased with the relative bar width. In addition, rectangular submerged breakwaters demonstrated a better reflection effect than the trapezoidal submerged breakwaters, and the triangular submerged breakwaters demonstrated a poor reflection effect.

Keywords: Bragg resonance; reflection coefficient; porous submerged breakwaters; horizontal seabed; flume experiments

Citation: Xu, W.; Chen, C.; Htet, M.H.; Sarkar, M.S.I.; Tao, A.; Wang, Z.; Fan, J.; Jiang, D. Experimental Investigation on Bragg Resonant Reflection of Waves by Porous Submerged Breakwaters on a Horizontal Seabed. *Water* **2022**, *14*, 2682. https://doi.org/10.3390/w14172682

Academic Editors: Chih-Hua Chang, Ruey-Syan Shih and Der-Chang Lo

Received: 2 August 2022
Accepted: 26 August 2022
Published: 29 August 2022

1. Introduction

Bragg resonance caused by a wave passing through undulating terrain can reflect the partial wave energy back to the sea and enhance the offshore side wave energy density, which can play a role in mitigating coastal erosion to a certain extent and provide a new idea for wave energy generation. Bragg and Bragg [1] discovered Bragg resonance when they used X-rays to study two parallel crystal structures. Since Davies [2] introduced Bragg resonance to water waves, its interaction between surface water waves and periodically undulating seabed topography has become an important topic in the field of water wave hydrodynamics. Bragg resonance of waves exists when the wavelength of the undulating seabed topography is an integral multiple of half of the incident wavelength, as shown in Figure 1. Based on Bragg resonance, the undulating seabed topography can effectively reflect the waves to protect the coast [3–13].

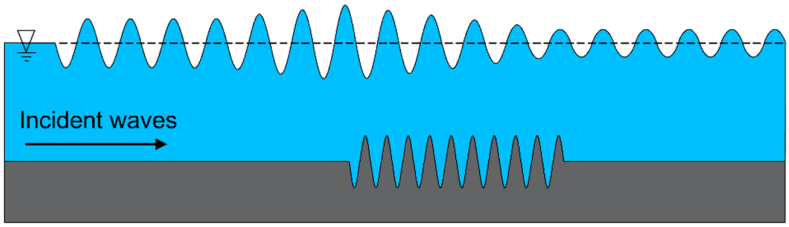

Figure 1. Schematic sketch of the Bragg resonant reflection of water waves.

When researching Bragg resonance theory, Davies and Heathershaw [14] applied perturbation theory to study the two-dimensional Bragg resonance of waves propagating on a sinusoidal rippled bottom, which contains surface incident waves, surface reflected waves, and topographic waves. Mei [15] explained a theory that sandbars can induce a strong reflection once the Bragg resonance condition is met. Guazzelli et al. [16] found that when the seabed topography was composed of two sine waves with different wavelengths, the frequency band caused by wave Bragg resonance became wider. Rey et al. [17] also applied the extended multi-scale method to study the characteristics of Bragg resonance, and derived the theoretical solution of subharmonic resonance caused by the interaction between free surface waves and topographic waves. Liu and Yue [18] implemented the high-order spectrum method to establish the Bragg resonance model of the interaction between waves and periodic undulating terrain, and pointed out that as the free wave surface components increased, the characteristics of Bragg resonance become complex, which includes harmonic and sub-harmonic resonance. Bragg resonance contains different wave and topographic parameters. According to its occurrence conditions, Liu and Yue [18] divided it into class I, class II, and class III. Peng et al. [19] relied on physical model experiments to confirm the existence of class III Bragg resonance. In addition, the triad resonance among free-surface waves, rippled bottoms, and ambient flow was further understood by applying multiple-scale expansion perturbation analysis and was captured by implementing flume experiments under critical flow conditions for resonant wave components [20]. Yu [21] studied the phenomenon and mechanism of the downshift of the primary frequency of Bragg resonance based on the wave numerical model of the higher-order spectral method and flume experiments, and Peng et al. [22] used this basis to deduce the theoretical solution of the downshift of the wave frequency of Bragg resonance. In conclusion, the occurrence conditions, resonant characteristics, resonant primary frequency, reflection coefficient, and reflection bandwidth of Bragg resonance has been comprehensively studied, which provides a basis for applying it to the coastal protection of submerged breakwaters.

In a study of the applications of Bragg resonance, Bailard et al. [23] proposed that Bragg resonant submerged breakwaters could be a new method for protecting the coast from waves. The effects of parameters such as section shapes, bar height, bar width, number of bars, and seabed slope on Bragg reflection were investigated by applying theoretical analysis and numerical simulation methods [24–30]. Tang and Huang [31] found that submerged breakwaters with sinusoidal sections presented the strongest reflection on the waves, but submerged breakwaters with rectangular, trapezoidal, and other sections could be added to simplify the construction process. Hsu et al. [32] studied the interaction characteristics between regular waves and submerged breakwaters with rectangular sections in wave flumes, and found that the maximum reflection did not appear where the ratio of the topographic wavelength to incident wavelength equaled 1/2, but shifted to a smaller value, as the theory did not consider viscous and nonlinear effects. Moreover, Ouyang et al. [33] applied a numerical simulation and found that a certain degree of reflection occurred when the breakwater spacing was about 1/4 of the incident wavelength. Liu et al. [34] studied the wave reflection and transmission coefficients during different wave periods and wavelengths with sinusoidal breakwaters, and also comprehensively considered oblique and forward incident waves. Yueh et al. [35] analyzed Bragg reflection of water waves

on submerged wavy plate breakwaters, and found that the wave reflection effect of wavy plate breakwaters was better than that of the horizontal plate. This research can provide adequate analysis and sufficient guidance for applications of submerged breakwaters based on Bragg resonance intended to protect the coast.

In addition, the Bragg reflection of porous submerged breakwaters is also considered in practical engineering, and these gaps are more conducive to water exchange and fish survival. At the same time, there is a significant effect on Bragg resonance. Mase et al. [36,37] developed a time-dependent wave equation for waves propagating over permeable rippled beds that considered the effects of porous media and analyzed the influence of seabed permeability on Bragg reflection. Zhang et al. [25] applied the numerical method to study the wave motion and seabed response around multiple permeable submerged breakwaters on a horizontal seabed. Ni and Teng [29,30] derived a modified mild-slope equation for water wave propagation over a porous seabed and studied the effects of permeability, height, width, and number of porous rectangular and trapezoidal bars on Bragg resonance, respectively, which were fixed on a sloping permeable seabed. Mohapatra et al. [38] investigated the Bragg scattering of surface waves by using a slender pile-supported submerged wavy porous plate and applying the numerical model, while including the assumption of small amplitude water wave theory. In conclusion, Chinese and foreign researchers have studied the influence of parameters such as bar size, as well as bar section shapes and layout on Bragg resonance, which provides a basis for enhancing the resonance strength and optimizing configuration. However, most research is based on theoretical analysis and numerical simulation, and few experimental studies focus on the permeability of Bragg submerged breakwaters.

In this study, Bragg resonant reflection on porous submerged breakwaters is studied by conducting a series of flume experiments that provide a reference for the theoretical and numerical results. A detailed analysis of the permeability, relative width, relative height, and section shapes of bars on Bragg resonant reflection is presented based on experimental data. In order to help readers to clearly understand the experimental process, some detailed experiment steps are introduced in Section 2, including the wave flume, porous bars, wave parameters, and experimental conditions. In Section 3, the influence of several important parameters, such as the permeability, relative width, relative height, and section shapes of bars on the Bragg resonant reflection are discussed and compared with other studies. Finally, the conclusions of this paper are discussed in Section 4.

2. Experimental Setup and Conditions

2.1. Wave Flume and Porous Submerged Breakwaters

The Bragg resonant reflection of porous submerged breakwaters was measured using the wave flume (70 m long, 1.2 m wide, and 1.7 m deep) at the Zhejiang Institute of Hydraulics and Estuary. The flume was equipped with a servo motor to generate regular and irregular waves with different wave spectra, while a porous wave absorber with a slope of 1:7, composed of grids and floating foam plates was installed at the end of the flume to absorb the incident wave energy. The porous bars composed of steel wire mesh and filler blocks were fixed in the test section of the flume. Furthermore, the DJ 800 sensor data acquisition system developed by the Chinese Institute of Water Resources and Hydropower Research was used to measure the wave parameters. The water surface elevations around the bars were measured by implementing six capacitance wave gauges, identified as WG.1–6, as shown in Figure 2. The method that Goda and Suzuki [39] proposed was applied to separate the incident and reflected waves. The spacing between WG.1 and WG.2 was set to 0.2 m, and the spacing between WG.2 and WG.3 was set to 0.3 m. The typical time histories of the free surface elevations are shown in Figure 3, where the stable surface elevations are between T_1 and T_2. The sampling interval of the wave gauges was 0.02 s, and each sampling time was 81.92 s. In order to ensure the reliability of the experiment, these gauges were calibrated in a small water tank before the tests and each case was repeated three times, after which the average values of the results were taken.

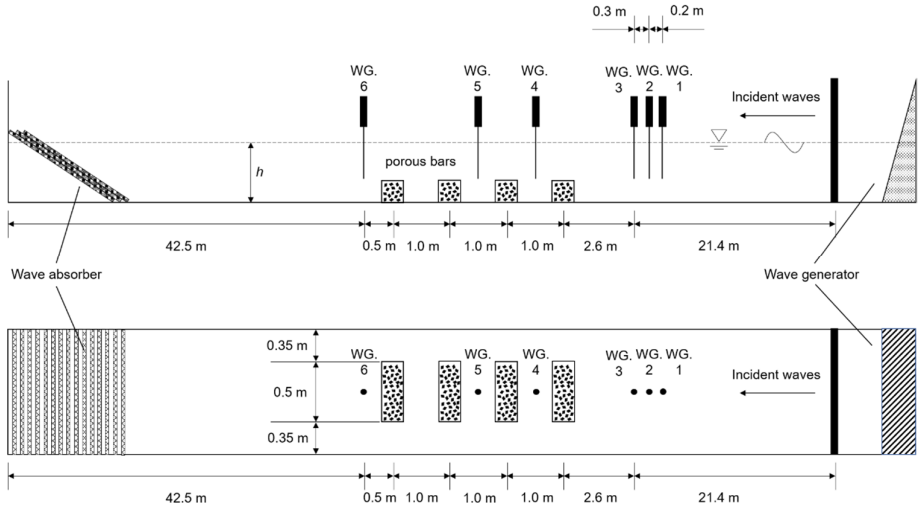

Figure 2. Sketch of experimental setup in side view and plan view.

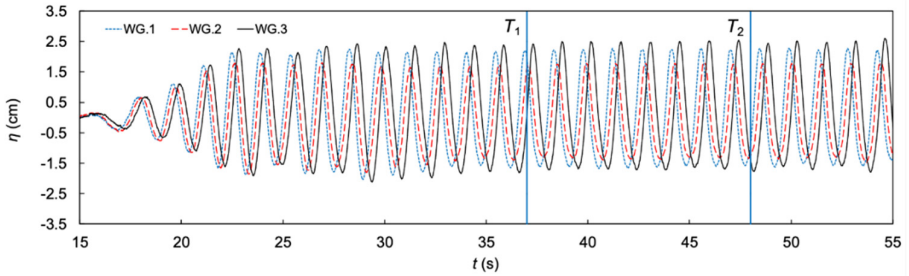

Figure 3. Time histories of free surface elevations η measured by WG.1−3.

The spacing between the submerged breakwaters with rectangular, triangular, and trapezoidal sections was set to 1m, which were composed of prefabricated alloy cages and different fillers, as shown in Figures 4–6. The alloy cage frame was made of aluminum, and the specific parameters are shown in Figure 7 and Table 1, where h is the water depth, B is the bar width, B_0 is the short bottom edge of the trapezoidal bars, D is the bar height, and S is the spacing of the two adjacent bars.

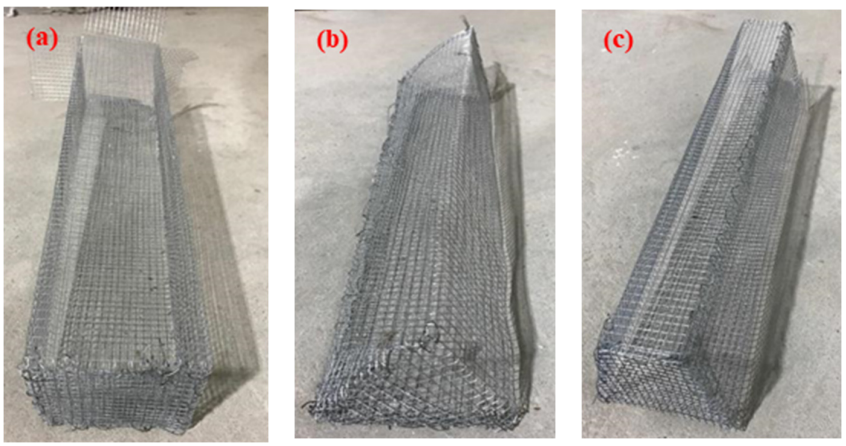

Figure 4. Alloy cages with different section shapes ((**a**) rectangle; (**b**) triangle; (**c**) trapezoid).

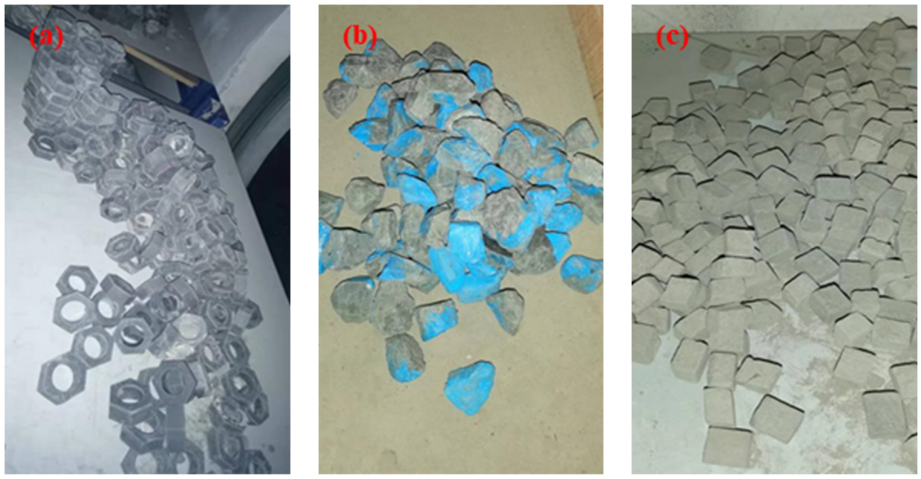

Figure 5. Different fillers ((**a**) filler A; (**b**) filler B; (**c**) filler C).

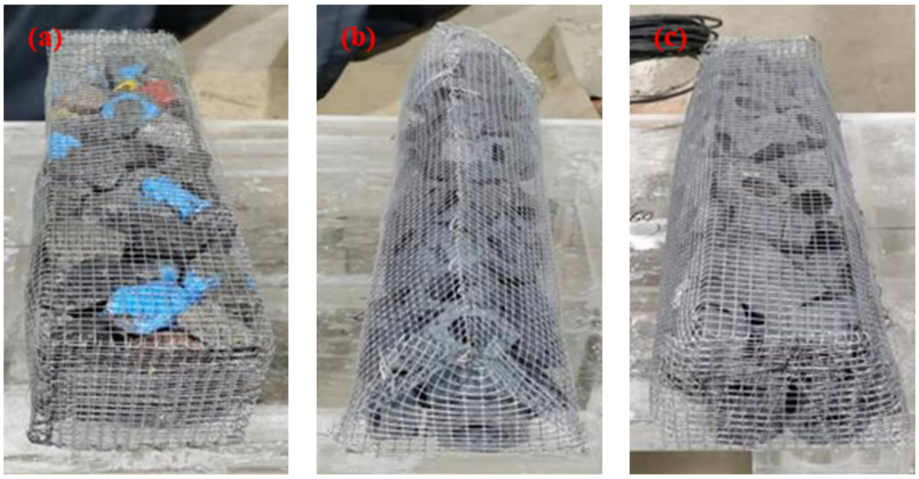

Figure 6. Simplified models of submerged breakwaters ((**a**) rectangle; (**b**) triangle; (**c**) trapezoid).

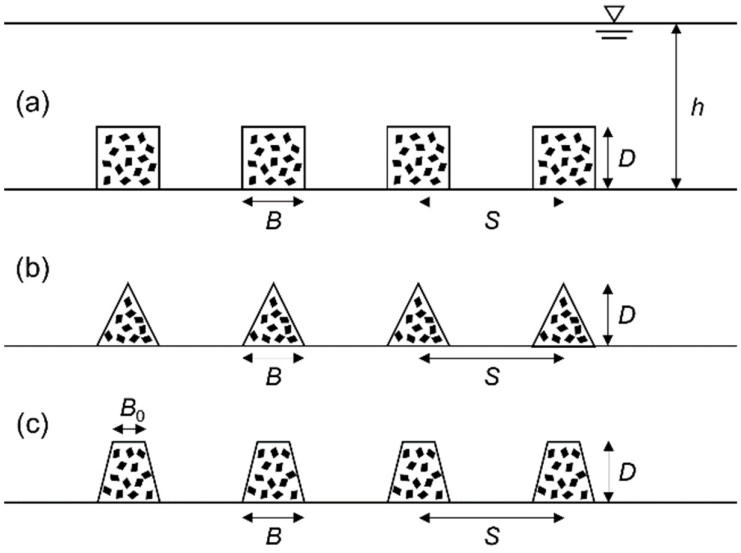

Figure 7. Sketch of porous submerged breakwaters with different section shapes and equal spacing ((**a**) rectangle; (**b**) triangle; (**c**) trapezoid. ***h*** is the water depth, ***B*** is the bar width, B_0 is the short bottom edge of the trapezoidal bars, ***D*** is the bar height, and ***S*** is the spacing of the two adjacent bars).

Table 1. Size of porous submerged breakwaters.

Section Shapes	Long (m)	B (m)	D (m)	B_0 (m)	S (m)
Rectangle	0.5	0.1	0.1	-	1.0
Triangle	0.5	0.1	0.1	-	1.0
Trapezoid	0.5	0.1	0.1	0.06	1.0

The permeability of the porous submerged breakwaters was determined by applying the drainage method [40]. In order to reduce the measured error resulting from the fillers, they were soaked in water for more than 5 h before measurement. At first, an appropriate amount of water was added into the container, and the volume was recorded as $\boldsymbol{V_1}$. Next, the fillers were put into the container so they were flush with the water surface, and the volume was recorded as $\boldsymbol{V_2}$. Then, the permeability of the porous submerged breakwaters $\boldsymbol{\varphi}$ can be expressed as

$$\boldsymbol{\varphi} = \boldsymbol{V_1}/\boldsymbol{V_2} \quad (1)$$

where $\boldsymbol{V_1}$ is the volume of water in the initial state in cubic centimeters (cm^3), and $\boldsymbol{V_2}$ is the total volume of the filler flush with the water surface in cubic centimeters (cm^3).

Finally, the permeability of filler A was 68.85%, filler B was 49.81%, and filler C was 31.26%, as shown in Table 2.

Table 2. The permeability of the fillers.

Fillers	V_1 (cm^3)	V_2 (cm^3)	φ (%)
A	30,937.48	44,934.61	68.85
B	29,186.32	58,595.26	49.81
C	32,370.26	103,551.70	31.26

2.2. Wave Parameters and Experimental Conditions

The regular wave was employed as the incident wave for this experiment, and the water depth $\boldsymbol{h}$, wave period $\boldsymbol{T}$, and wave height $\boldsymbol{H}$ were the main parameters controlling wave making. The wave height was 0.04 m, and the water depth was 0.25 m, 0.30 m, and 0.40 m, respectively. The wave period $\boldsymbol{T}$ varied with the ratio of twice the distance between the adjacent submerged breakwaters to the wavelength is 2 $\boldsymbol{S/L}$, and 2 $\boldsymbol{S/L}$ is equal to 0.80, 0.86, 0.91, 0.94, 0.97, 1.00, 1.04, 1.12, and 1.21. The main factors affecting the Bragg resonant reflection are the permeability, height, width, spacing, section shape, and number of submerged breakwaters. In this study, the number of bars $\boldsymbol{N}$ was fixed at 4, and the effects of permeability $\boldsymbol{\varphi}$, relative width $\boldsymbol{B/S}$, relative height $\boldsymbol{D/h}$, and section shapes on the Bragg resonant reflection were investigated respectively, as shown in Table 3.

Table 3. Experimental cases and conditions.

Case	h (m)	T (s)	H (m)	φ (%)	Section Shapes	B (m)	D (m)	N
1	0.25	1.20–1.70	0.04	0, 31.26, 49.81, 68.85, 100	Rectangle	0.2	0.1	4
2	0.25	1.20–1.70	0.04	68.85	Rectangle	0.1, 0.2, 0.3	0.1	4
3	0.25, 0.30, 0.40	1.05–1.70	0.04	68.85	Rectangle	0.3	0.1	4
4	0.25	1.20–1.70	0.04	68.85	Rectangle, triangle, trapezoid	0.2	0.1	4

3. Experimental Results

It is widely known that Bragg reflection will occur when the ratio of double submerged breakwaters spaced to wavelength 2 $\boldsymbol{S/L}$ is near an integral multiple [14,15]. Therefore, this

phenomenon and the change in reflectivity are discussed using the parameter 2 S/L. This part analyzes the correlation between φ, B/S, D/h, section shapes, and the wave reflection coefficient K_R, which is expressed by the ratio of the amplitude of the reflected wave to that of the incident wave.

3.1. Influence of Bar Permeability on Bragg Resonant Reflection

Whether periodic submerged breakwaters are permeable will change the attenuation mechanism of the waves propagating on varying bottom structures. A certain bar elevation was selected in the test to ensure that wave breaking would not occur. In this section, the influence of submerged breakwater permeability on Bragg resonant reflection is discussed in detail, and some observations during the tests are presented. In addition, the reflection coefficients at different permeabilities measured in this study were compared with the experimental study conducted by Mase et al. [36]. The controlled parameters were given as N = 4, B = 0.2 m, D = 0.1 m, S = 1.0 m, h = 0.25 m, and H = 0.04 m. The submerged breakwater section was rectangular. We let 2 S/L vary from 0.8 to 1.21, and T varied from 1.2s to 1.7s. The permeability of the submerged breakwater was 0 (solid bars), 31.26%, 49.81%, 68.85%, and 100% (no bar), respectively.

The experimental results are plotted in Figure 8. This indicates that the Bragg resonant reflection coefficient first increased and then decreases in the range of 2 S/L 0.8–1.21, and its peak value is near 0.95. This agrees with the results of Liu et al. [34], Mase et al. [36], Heathershaw [41], and Chang et al. [42]. Theoretically, the peak value of Bragg resonance dominant frequency appeared at a 2 S/L equal to 1, and this difference could be explained by the downshift of wave frequency for Bragg resonance [22]. Another phenomenon that could be observed is that the Bragg resonant reflection coefficient decreased with the increased permeability. The same conclusion could be obtained from the numerical results of Ni and Teng [29]. When the permeability of submerged breakwaters was 0, 31.26%, 49.81%, and 68.85%, the measured peak reflection coefficient was 0.287, 0.210, 0.171, and 0.152, respectively. When there was no bar on the bottom bed, there was still a small reflection coefficient, which could be due to the errors as a result of the process of separating the measured waves into incident and reflected waves. The calculations and analyses showed that the reflection coefficients of the submerged breakwaters with a permeability of 31.26%, 49.81%, and 68.85% were reduced by 26.83%, 40.42%, and 47.04%, respectively, compared with the submerged breakwaters with a permeability of 0. Furthermore, it was found that a slowing trend occurred when the Bragg resonant reflection coefficient peak decreased with the increased permeability, as shown in Figure 9.

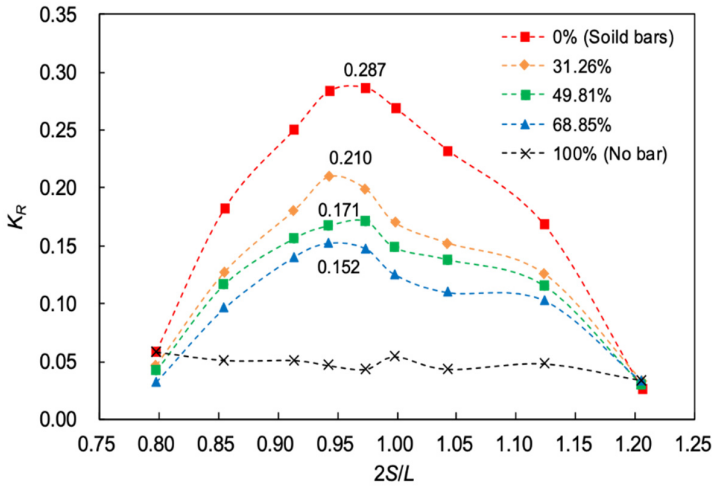

Figure 8. Influence of submerged breakwater permeability φ on Bragg resonant reflection, rectangle, N = 4, B = 0.2 m, S = 1.0 m, h = 0.25 m, and H = 0.04 m.

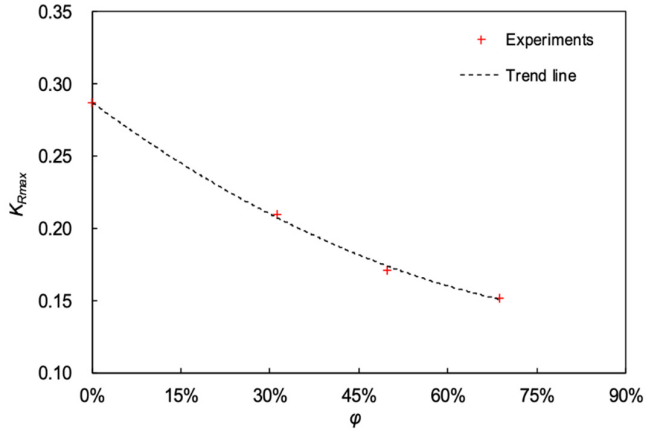

Figure 9. Variation of Bragg resonant reflection coefficient peak K_{Rmax} with permeability φ.

Figure 10 shows the results from this experiment compared with those of Mase et al. [36]. Mase et al. [36] employed porous trapezoidal submerged breakwaters on a flat bottom terrain, and the number of bars was fixed at 4. The solid and dotted lines in Figure 10 represent the theoretical predicted value under impermeable and permeable conditions, respectively. The hollow squares and circles represent the test values under impermeable and permeable conditions measured by Mase et al. [36]. The Bragg resonant reflection coefficient of permeable bars was smaller than that of the impermeable bars and decreased with the increased permeability. This was because when waves propagate on the bottom bed of the submerged breakwaters, some fluids passed through the pores of the submerged breakwaters, which weakened the Bragg resonant reflection.

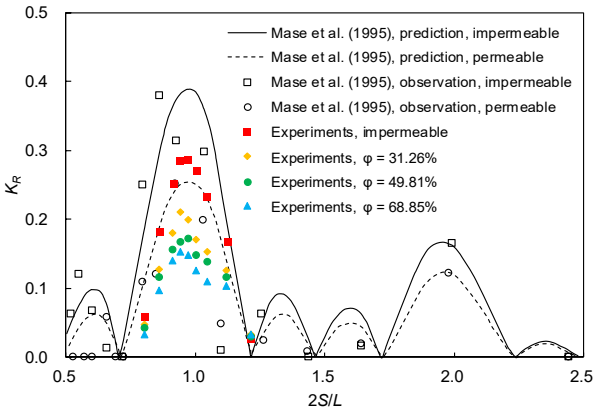

Figure 10. Comparison of experimental values of porous bars on the horizontal seabed (Mase et al. [36]).

3.2. Influence of the Relative Width on Bragg Resonant Reflection

This section discusses the influence of the relative width of submerged breakwaters B/S on the Bragg resonant reflection coefficient, which is defined by the ratio of a single bar width B to spacing between two adjacent bars S. In this study, we set N = 4, φ = 68.85%, D = 0.1 m, S = 1.0 m, h = 0.25 m, and H = 0.04 m. The submerged breakwaters were rectangular and T varied from 1.2s to 1.7s. The values of B/S were 0.1, 0.2, and 0.3, respectively. The reflection coefficient K_R against 2 S/L for 2 S/L varying from 0.8 to 1.21 was calculated and is presented in Figure 11. When 2 S/L was near 1, the Bragg resonant reflection coefficient reached its maximum and there was a trend of first increasing and then decreasing to near 1. When the relative bar width was 0.1, 0.2, and 0.3, respectively, the measured peak reflection coefficient was 0.119, 0.152, and 0.162. The situation without submerged breakwaters has been described in the previous section. The calculations and

analyses show that the peak reflection coefficient with a relative bar width of 0.2 and 0.3 increased by 27.73% and 36.13% compared with the relative bar width of 0.1.

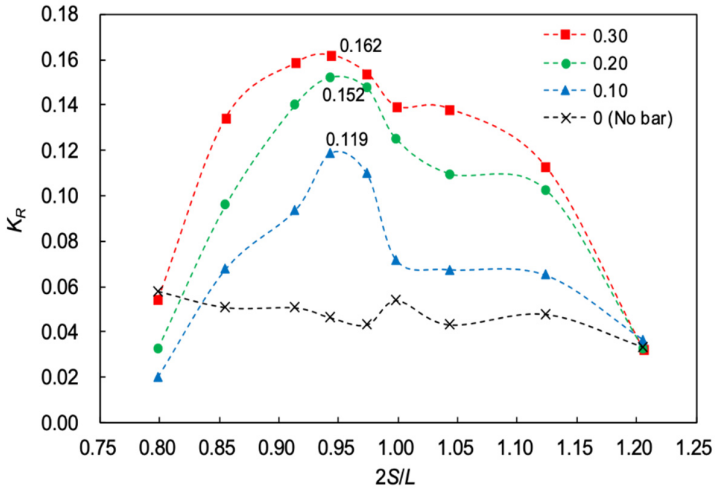

Figure 11. Influence of the relative width B/S on Bragg resonant reflection, rectangle, N = 4, φ = 68.85%, S = 1.0 m, h = 0.25 m, and H = 0.04 m.

The relationship between the peak value of Bragg resonant reflection coefficient and B/S is plotted in Figure 12, and the results of Chang et al. [42], Ni and Teng [29], and this test are compared. Different views have been expressed regarding this point. Chang [42] and Tsai [43] pointed out that when submerged breakwaters had a smaller relative width, in other words, when the distance between submerged breakwaters was larger, the Bragg reflection phenomenon was more obvious and the peak reflection coefficient was larger. However, Liu et al. [28], and Ni and Teng [29], found that a particular value of the bar width could maximize the Bragg resonant reflection. When the relative bar width increased from B/S = 0.1 to B/S = 0.5, the peak value of the Bragg resonant reflection coefficient increased gradually. However, when the relative width continued to increase from B/S = 0.5 to B/S = 0.9, the peak value of the Bragg resonant reflection coefficient decreased instead, as shown in Figure 12. Furthermore, this coefficient increased with the increased relative width in the range of 0.1–0.3. This is somewhat consistent with the numerical results from Liu et al. [28], and Ni and Teng [29]. Moreover, additional experimental conditions should be implemented to prove this conclusion.

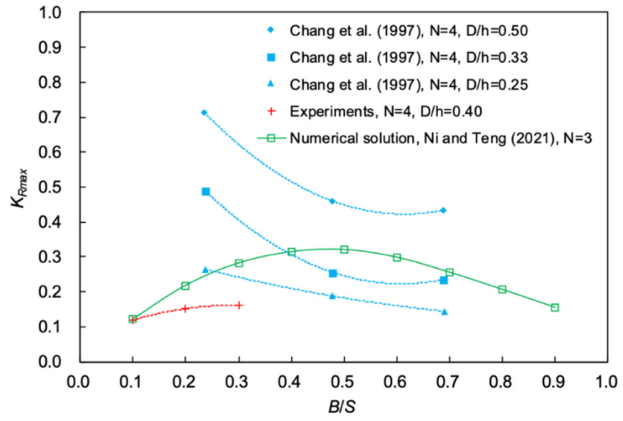

Figure 12. Comparison of Bragg resonant reflection coefficient peak K_{Rmax} with relative width B/S (Chang et al. [42], Ni and Teng [29]).

3.3. Influence of the Relative Height on Bragg Resonant Reflection

This section describes the influence of relative height on Bragg resonant reflection. Figure 13 shows the measurement results of the Bragg resonant reflection coefficient that varies with the relative bar height D/h, where the porous submerged breakwater section is rectangular, N = 4, φ = 68.85%, B = 0.3 m, S = 1.0 m, and H = 0.04 m. The relative height D/h had three values of 0.25, 0.33, and 0.40, where the bar height D was fixed at 0.1 m, and the relative bar height varied by changing the water depth h. Moreover, 2 S/L varied from 0.80 to 1.21, and T increased from 1.05 s to 1.70 s. Similarly, the overall trend increased first and then decreased, and the maximum reflection coefficient appeared when the incident wavelength was almost twice the spacing between the two adjacent bars. Moreover, according to the experimental results, when the relative height was in the range of 0–0.40, the Bragg resonant reflection was positively correlated with the relative bar height, that is, a higher relative height indicated a greater reflection coefficient. When the relative height was 0.25, 0.33, and 0.40, the peak values of the Bragg resonant reflection coefficient were 0.078, 0.130, and 0.162, respectively. The peak reflection coefficient with a relative height of 0.33 and 0.40 was twice and two-thirds higher than that with a relative bar height of 0.25.

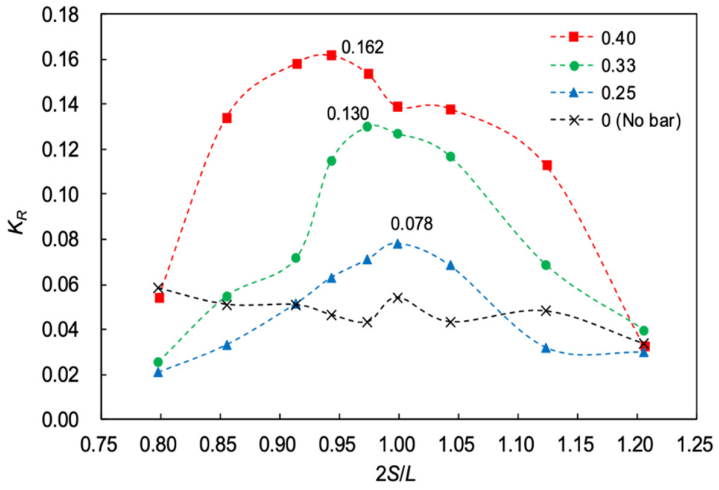

Figure 13. Influence of the relative height D/h on the Bragg resonant reflection, rectangle, N = 4, φ = 68.85%, B = 0.3 m, S = 1.0 m, and H = 0.04 m.

According to the numerical calculations and experimental results of Guazzelli et al. [16] and Chang et al. [42], when the amplitude of the sand ripple bottom bed increased, the intensity of the Bragg reflection and its reflectivity bandwidth could be increased. Chang et al. [42] pointed out that the increased bar height contributed to the increased overall reflectivity in the research results related to the equally spaced series of submerged breakwaters.

Figure 14 shows the results of the comparisons with previous studies. The hollow label is the experimental results of Davies and Heathershaw [14] in the sinusoidal sand ripple bottom bed, and the solid label is the experimental results of the rectangular series of submerged breakwaters by Chang et al. [42], both of which did not consider permeability. The red plus sign was the test results of a series of rectangular submerged breakwaters with a permeability of 68.85%. The graph shows that the peak reflection coefficient increased with the increase in the relative height of the submerged breakwaters or the sand ripples, whether it was the sinusoidal sand ripple bed and the rectangular submerged breakwaters, while not considering permeability, or the rectangular submerged breakwaters, while considering permeability. The reason is that when the relative height of submerged breakwaters or sand ripples increased, the water depth at the top of the bars decreased. When the waves propagated on the undulating topography, the interaction with the bars or sand ripples

intensified, so the peak reflectivity also increased. However, a slowing trend occurred when the Bragg resonant reflection coefficient peak increased with the increased relative bar height.

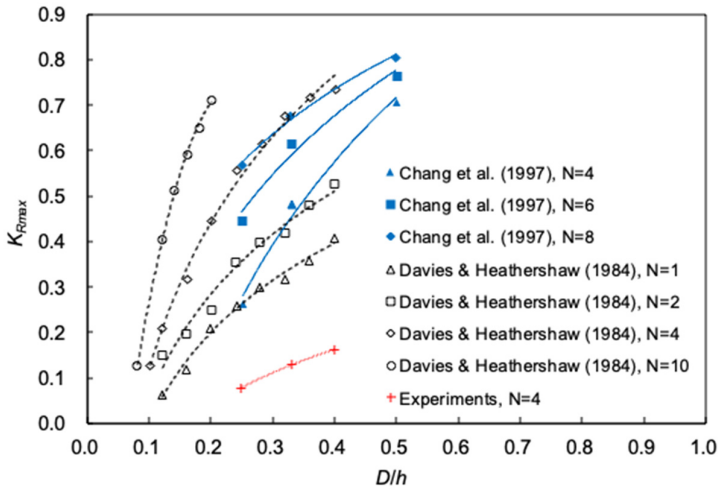

Figure 14. Comparison of the Bragg resonant reflection coefficient peak K_{Rmax} with the relative height D/h (Chang et al. [42], Davies and Heathershaw [14]).

3.4. Influence of Section Shapes of Bars on Bragg Resonant Reflection

Finally, the influence of different submerged breakwater section shapes on the Bragg resonant reflection is investigated. If N = 4, B = 0.2 m, D = 0.1 m, S = 1.0 m, φ = 68.85%, h = 0.25 m, and H = 0.04 m, the section shapes of submerged breakwaters are fixed as a rectangle, triangle, and trapezoid. Moreover, 2 S/L varied from 0.8 to 1.21, and T varied from 1.2 s to 1.7 s. The results are plotted in Figure 15, which shows the experimental values of the Bragg resonant reflection coefficient with different section shapes of bars. The variation of the reflection coefficient with $2S/L$ was the same as in the previous three sections. Moreover, it was shown that in the same conditions, the rectangular submerged breakwaters had the best Bragg resonant reflection coefficient with a value of 0.162. Moreover, the trapezoidal submerged breakwaters were ranked second with a reflection coefficient of 0.133, while the triangular ones had a poor reflection effect with a value of 0.107.

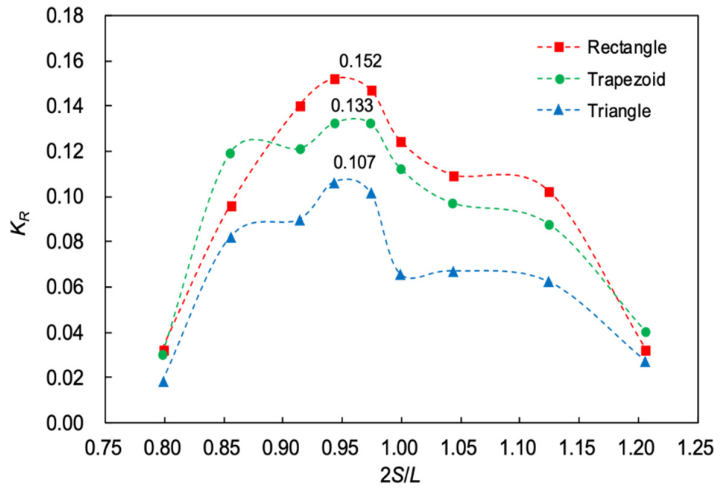

Figure 15. Influence of section shapes of bars on Bragg resonant reflection, N = 4, B = 0.2 m, D = 0.1 m, S = 1.0 m, φ = 68.85%, h = 0.25 m, and H = 0.04 m.

As shown in Figure 16, the numerical results of the rectangular, trapezoidal, and triangular bars from Cho et al. are represented by the red, green, and blue dotted lines,

respectively. [5]. In addition, the red square, green circle, and blue triangle represented the test values for the rectangular, trapezoidal, and triangular submerged breakwaters, respectively. According to the test results, the trend of the graphics was consistent with the numerical results from Cho et al. [5]. The rectangular section had a better reflection effect than the trapezoidal section, and the triangular section had a poor one. The small reflection coefficient in our test was mainly due to the influence of the permeability of the submerged breakwaters, while Cho et al.'s research focus was solid submerged breakwaters. In addition, this was also related to the relative width and height of the submerged breakwaters. In the work of Cho et al. [5], the primary frequency of the rectangular submerged breakwaters appears where $2S/L$ was close to 0.8, and the primary frequency had an obvious downshift, which was not obvious in this experiment.

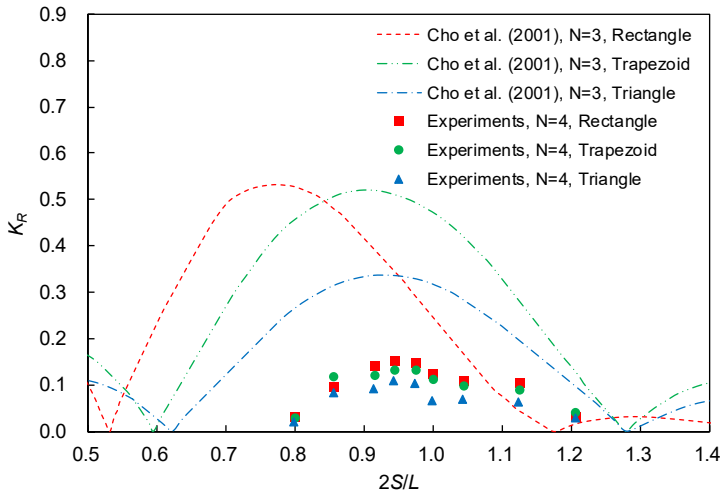

Figure 16. Comparison of the Bragg resonant reflection coefficient K_R with section shapes of bars (Cho et al. [5]).

It must be mentioned that there were also some improvements that needed to been paid more attention in this experiment. The experimental layout restricted the length of the models and did not cover the full width the flume, which would induce wave scattering effects emanating from the end sections of the submerged models that could affect reflected wave. This study mainly focused on the influence of the porous submerged breakwaters on the Bragg resonant reflection based on the overall trend of the Bragg resonant reflection coefficient, so the specific measurement value had little influence. Similarly, compared with previous research results, the incompletely consistent parameters, such as bar permeability, number of bars, relative width, and wave period, did not affect the overall trend of the experimental results.

4. Conclusions

In order to further study the Bragg resonant reflection of waves propagating on porous submerged breakwaters, flume experiments were applied to investigate the effects of permeability, relative width, relative height, and section shapes of porous submerged breakwaters on Bragg resonant reflection. The results have a lot in common with previous research, and additional detailed results were found.

When the ratio of the double adjacent submerged breakwater spacing to wavelength nears 1, the reflection coefficient reaches its peak, and its primary frequency shifts down to a certain extent. Bragg resonant reflection coefficient increases with the decreasing permeability and increasing relative height of the submerged breakwaters. However, a slowing trend occurs when the Bragg resonant reflection coefficient peak decreases with the increased permeability and increases with the increased relative height. This coefficient increases with the increased relative width in the range of 0.1–0.3. This somewhat verifies

the numerical solutions from Liu et al. [28], as well as Ni and Teng [29], that the reflection coefficient first increases and then decreases with the relative width. Among the submerged breakwaters with rectangular, triangular, and trapezoidal section shapes, the rectangular submerged breakwaters show a better Bragg resonant reflection effect and the trapezoidal ones are ranked second. The triangular ones have a poor reflection effect.

Author Contributions: Conceptualization, methodology, validation, formal analysis, writing—original draft preparation, W.X.; investigation, Z.W. and J.F.; writing—review and editing, M.H.H. and M.S.I.S.; supervision and funding acquisition, C.C., A.T. and D.J. All authors have read and agreed to the published version of the manuscript.

Funding: This research was funded by the National Key Research and Development Program of China (grant Nos. 2022YFE0104500 and 2020YFD0900701) and the Research Project on Representative Islands Platform for Resources, Ecology, and Sustainable Development (grant Nos. 2029999 and 220005).

Data Availability Statement: Not applicable.

Acknowledgments: The authors thank the anonymous reviewers for their constructive comments.

Conflicts of Interest: The authors declare no conflict of interest.

References

1. Bragg, W.H.; Bragg, W.L. The Reflection of X-rays by Crystals. *Proc. R. Soc. London Ser. A Math. Phys. Eng. Sci.* **1913**, *88*, 428–438. [CrossRef]
2. Davies, A.G. The Reflection of Wave Energy by Undulations on the Seabed. *Dyn. Atmos. Oceans* **1982**, *6*, 207–232. [CrossRef]
3. Mei, C.C.; Hara, T.; Naciri, M. Note on Bragg Scattering of Water Waves by Parallel Bars on the Seabed. *J. Fluid Mech.* **1988**, *186*, 147–162. [CrossRef]
4. Kirby, J.T.; Anton, J.P. Bragg Reflection of Waves by Artificial Bars. In Proceedings of the 22nd International Conference on Coastal Engineering, Delft, The Netherlands, 2–6 July 1990; pp. 757–768.
5. Cho, Y.S.; Yoon, S.B.; Lee, J.I.; Yoon, T.H. A Concept of Beach Protection with Submerged Breakwaters. *J. Coast. Res.* **2001**, *34*, 671–678.
6. Hsu, T.W.; Chang, H.K.; Tsai, L.H.; Li, Y.X. Experiments on the Bragg Reflection of Waves by Different Types of Artificial Bars. In Proceedings of the 11th International Offshore and Polar Engineering Conference, Stavanger, Norway, 17–22 June 2001; pp. 601–606.
7. Hsu, T.W.; Chang, H.K.; Tsai, L.H. Bragg Reflection of Waves by Different Shapes of Artificial Bars. *China Ocean Eng.* **2002**, *16*, 343–358.
8. Hsu, T.W.; Tsai, L.H.; Huang, Y.T. Bragg Scattering of Water Waves by Multiply Composite Artificial Bars. *Coast Eng. J.* **2003**, *45*, 235–253. [CrossRef]
9. Hsu, T.W.; Hsiao, S.C.; Ou, S.H.; Wang, S.K.; Yang, B.D.; Chou, S.E. An Application of Boussinesq Equations to Bragg Reflection of Irregular Waves. *Ocean Eng.* **2007**, *34*, 870–883. [CrossRef]
10. Jeon, C.H.; Cho, Y.S. Bragg Reflection of Sinusoidal Waves Due to Trapezoidal Submerged Breakwaters. *Ocean Eng.* **2006**, *33*, 2067–2082. [CrossRef]
11. Wang, S.K.; Hsu, T.W.; Tsai, L.H.; Chen, S.H. An Application of Miles' Theory to Bragg Scattering of Water Waves by Doubly Composite Artificial Bars. *Ocean Eng.* **2006**, *33*, 331–349. [CrossRef]
12. Tsai, L.H.; Kuo, Y.S.; Lan, Y.J.; Hsu, T.W.; Chen, W.J. Investigation of Multiply Composite Artificial Bars for Bragg Scattering of Water Waves. *Coast Eng. J.* **2011**, *53*, 521–548.
13. Gao, J.L.; Ma, X.Z.; Dong, G.H.; Chen, H.Z.; Liu, Q.; Zang, J. Investigation on the Effects of Bragg Reflection on Harbor Oscillations. *Coast. Eng.* **2021**, *170*, 103977. [CrossRef]
14. Davies, A.G.; Heathershaw, A.D. Surface-wave Propagation over Sinusoidally Varying Topography. *J. Fluid Mech.* **1984**, *144*, 419–443. [CrossRef]
15. Mei, C.C. Resonant Reflection of Surface Water Waves by Periodic Sandbars. *J. Fluid Mech.* **1985**, *152*, 315–335. [CrossRef]
16. Guazzelli, E.; Rey, V.; Belzons, M. Higher-order Bragg Reflection of Gravity Surface Waves by Periodic Beds. *J. Fluid Mech.* **1992**, *245*, 301–317. [CrossRef]
17. Rey, V.; Guazzelli, E.; Mei, C.C. Resonant Reflection of Surface Gravity Waves by One-dimensional Doubly Sinusoidal Beds. *Phys. Fluids.* **1996**, *8*, 1525–1530. [CrossRef]
18. Liu, Y.; Yue, D.K. On Generalized Bragg Scattering of Surface Waves by Bottom Ripples. *J. Fluid Mech.* **1998**, *356*, 297–326. [CrossRef]
19. Peng, J. *Influence Mechanism of Higher Order Nonlinearity on Gravity Wave Bragg Resonance*; Hohai University: Nanjing, China, 2020. (In Chinese)

20. Fan, J.; Zheng, J.H.; Tao, A.F.; Liu, Y.M. Upstream-propagating Waves Induced by Steady Current over A Rippled Bottom: Theory and Experimental Observation. *J. Fluid Mech.* **2021**, *910*, A49. [CrossRef]
21. Yu, H.F. *The Downshift Characteristics of Critical Frequency Research during Wave Bragg Resonance Processes*; Hohai University: Nanjing, China, 2016. (In Chinese)
22. Peng, J.; Tao, A.F.; Fan, J.; Zheng, J.H.; Liu, Y.M. On the Downshift of Wave Frequency for Bragg Resonance. *China Ocean Eng.* **2022**, *36*, 76–85. [CrossRef]
23. Bailard, J.A.; DeVries, J.; Kirby, J.T.; Guza, R.T. Bragg Reflection Breakwater: A New Shore Protection Method. *Coast. Eng.* **1990**, *1*, 1702–1715.
24. Chang, H.K.; Liou, J.C. Long Wave Reflection from Submerged Trapezoidal Breakwaters. *Ocean Eng.* **2007**, *34*, 185–191. [CrossRef]
25. Zhang, J.S.; Jeng, D.S.; Liu, P.F.; Zhang, C.; Zhang, Y. Response of a Porous Seabed to Water Waves over Permeable Submerged Breakwaters with Bragg Reflection. *Ocean Eng.* **2012**, *43*, 1–12. [CrossRef]
26. Ouyang, H.T.; Chen, K.H.; Tsai, C.M. Wave Characteristics of Bragg Reflections from a Train of Submerged Bottom Breakwaters. *J. Hydro-Environ. Res.* **2016**, *11*, 91–100. [CrossRef]
27. Zeng, H.; Qin, B.; Zhang, J. Optimal Collocation of Bragg Breakwaters with Rectangular Bars on Sloping Seabed for Bragg Resonant Reflection by Long Waves. *Ocean Eng.* **2017**, *130*, 156–165. [CrossRef]
28. Liu, H.W.; Zeng, H.D.; Huang, H.D. Bragg Resonant Reflection of Surface Waves from Deep Water to Shallow Water by a Finite Array of Trapezoidal Bars. *Appl. Ocean Res.* **2020**, *94*, 101976. [CrossRef]
29. Ni, Y.L.; Teng, B. Bragg Resonant Reflection of Water Waves by a Bragg Breakwater with Porous Rectangular Bars on a Sloping Permeable Seabed. *Ocean Eng.* **2021**, *235*, 109333. [CrossRef]
30. Ni, Y.L.; Teng, B. Bragg Resonant Reflection of Water Waves by a Bragg Breakwater with Porous Trapezoidal Bars on a Sloping Permeable Seabed. *Appl. Ocean Res.* **2021**, *114*, 102770. [CrossRef]
31. Tang, H.J.; Huang, C.C. Bragg Reflection in a Fully Nonlinear Numerical Wave Tank Based on Boundary Integral Equation Method. *Ocean Eng.* **2008**, *35*, 1800–1810. [CrossRef]
32. Hsu, T.W.; Lin, J.F.; Hsiao, S.C.; Ou, S.H.; Babanin, A.V.; Wu, Y.T. Wave Reflection and Vortex Evolution in Bragg Scattering in Real Fluids. *Ocean Eng.* **2014**, *88*, 508–519. [CrossRef]
33. Ouyang, H.T.; Chen, K.H.; Tsai, C.M. Investigation on Bragg Reflection of Surface Water Waves Induced by a Train of Fixed Floating Pontoon Breakwaters. *Int. J. Nav. Archit. Ocean Eng.* **2015**, *7*, 951–963. [CrossRef]
34. Liu, Y.; Li, H.J.; Zhu, L. Bragg Reflection of Water Waves by Multiple Submerged Semi-circular Breakwaters. *Appl. Ocean Res.* **2016**, *56*, 67–78. [CrossRef]
35. Yueh, C.Y.; Chuang, S.H.; Wen, C.C. Bragg Reflection of Water Waves Due to Submerged Wavy Plate Breakwater. *J. Hydro-Environ. Res.* **2018**, *21*, 52–59. [CrossRef]
36. Mase, H.; Oki, S.I.; Takeba, K. Wave Equation over Permeable Rippled Bed and Analysis of Bragg Scattering of Surface Gravity Waves. *J. Hydraul. Res.* **1995**, *33*, 789–812. [CrossRef]
37. Mase, H.; Kimura, A.; Sakakibara, H. Resonant Reflection and Refraction-diffraction of Surface Waves Due to Porous Submerged Breakwaters. *Coast. Eng. Proc.* **1996**, *15*, 2366–2376.
38. Mohapatra, A.K.; Vijay, K.G.; Sahoo, T. Bragg Scattering of Surface Gravity Waves by a Submerged Wavy Porous Plate. *Ocean Eng.* **2021**, *219*, 108273. [CrossRef]
39. Goda, Y.; Suzuki, T. Estimation of Incident and Reflected Waves in Random Wave Experiments. *Coast. Eng. Proc.* **1976**, *15*, 47. [CrossRef]
40. Harwalkar, V.R.; Kalab, M. Comparison of Centrifugation and Drainage Methods. *Milchwissenschaft* **1983**, *38*, 517–522.
41. Heathershaw, A.D. Seabed-wave Resonance and Sand Bar Growth. *Nature* **1982**, *296*, 343–345. [CrossRef]
42. Chang, H.K.; Hsu, T.W.; Lee, Y.H. Experimental Study of Waves Passing through Artificial Sandbars. In Proceedings of the 19th Ocean Engineering, Taichung, China, 17–18 November 1997; pp. 242–249. (In Chinese)
43. Tsai, L.H. *Bragg Reflection of Water Waves by a Series of Submerged Breakwaters*; National Cheng Kung University: Taichung, China, 2003. (In Chinese)